SUPPLEMENTARY INFORMATION FOR

"Identification and characterization of mitochondrial subtypes in *C. elegans* via analysis of individual mitochondria by flow cytometry"

Joseph R. Daniele[1], Kartoosh Heydari[2], Edgar A. Arriaga*[3] & Andrew Dillin[1]

1. Department of Molecular & Cellular Biology,

University of California, Berkeley

Berkeley, CA 94720

2. LKS Flow Cytometry Core, Cancer Research Laboratory,

University of California, Berkeley

Berkeley, CA 94720

3. Department of Chemistry,

University of Minnesota

Minneapolis, MN 55455

*** = Corresponding Author: arriaga@umn.edu**

Supplemental Experimental Procedures

Molecular Biology and Transgenic Worm Generation
Worms with blue fluorescent protein ("TagBFP" or "BFP") expressed exclusively in the muscle used a *myo-3p*::*MLS*::*BFP* which was created using pieces from five vectors: (1) the muscle specific promoter from the *myo-3* gene generously given to us by the Barbara Meyer Lab (pCFJ104), (2) the mitochondrial localization signal from the Fire lab *C. elegans* vector kit (pD96.32), (3) a codon optimized TagBFP generously given to us by the Abby Dernberg lab (pSK16)[1], and (4) the 3' UTR from the *unc-54* transcript also from the Fire lab *C. elegans* vector kit (pD96.32), (5) a vector backbone (pCFJ365) which included an *unc-119* rescue protein to identify successful DNA injections. The germline of late larval L4 worms was injected as described previously into strain *eg6703* (*unc-119(ed3) III; cxTi10816 IV;)* which was mutant for *unc-119*[2]. After injection worms that moved normally across the plate (or *unc-119* +) were picked and placed on new plates to enrich for worms with extrachromosomal arrays. Three extrachromosomal lines were isolated and used in this paper (referred to as lines #4, #8 and # 10).

Western Analysis
Protocols for Western sample preparation, blotting membranes, and membrane visualization were as described in [3]. Samples were prepared as described in the "*Mitochondrial Isolation and Flow Experiments"* portion of the "Experimental Section" in the main text and "boiled" (95º C) for 10 minutes in 2x Laemmli sample buffer (161-0737, BioRad) plus βME (M6250, Sigma) and Protease Inhibitor (539134, Calbiochem). All samples were run on 4–20% polyacrylamide ready gels (456-1096, BioRad).Samples prepared from lysates had protein concentration quantified (RC DC Protein Assay, 5000121 , BioRad) and equivalent amounts of subsequent fractions were loaded into each well. Primary antibodies used and their concentrations are listed below: mouse anti-MitoProfile® Total OXPHOS Rodent WB Antibody Cocktail (MS604, 1:2000), mouse anti-NDUFS3 (17D95, 1:2000), rabbit anti-Histone H3 (ab1791, 1:5000), and mouse anti-α-Tubulin (T6074, 1:10,000). Secondary antibodies included dye-conjugtated IRDye 800CW Donkey anti-Rabbit IgG and IRDye® 680RD Donkey anti-Mouse IgG, at a 1:20,000 dilution. Western images were acquired using a LiCor Odyssey and visualized using Image Studio Lite 3.1.

Live Worm Labeling and Confocal Microscopy
To label live worms (which were used to validate MLS::BFP labeling in the muscle) 2uL of liquid OP50 culture (normally used to seed NGM plates for culturing worms) was used to inoculate 1 mL of LB broth. This culture was then shaken at 37º C for 4 hours. MitoTracker Green (10 uL per 1 mL) of a 5 mM stock was then added to this culture and the tube was put at 37º C for another 4-6 hours. Cultures were then spun down at 4400 x G for 10 minutes (to remove any Mitotracker Green that was not taken up by the bacteria). These pellets were then resuspended with 500 uL of fresh, unlabeled, LB broth. This labeled culture was then seeded on NGM plates and allowed to dry overnight in a lightproof box (of note, all steps of this labeling used light-protected tubes to decrease the chances that the MitoTracker dye got bleached by light). Dry, seeded, plates were then used the next day when L4 staged worms were spotted on the plates for 1-2 hours at 20º C. After worm labeling, individual worms were taken off plates, put on a microscope slide and anesthetized in levamisole hydrochloride (10 mM) solution. A coverslip was added and sealed with nail polish and live slides were taken to the confocal for immediate imaging. Specimens were viewed on a Zeiss LSM700 Inverted confocal microscope, with constant acquisition settings when comparing specimens within a given experiment. Images in Figure S4A-B are maximum intensity projections (using the 'Processing' tab in Zen software) of stacks spanning the entire width of an anesthetized, unlabeled, transgenic animal.

Seahorse Measurements
Worm oxygen consumption ratio (OCR) was measured on a Seahorse XFe 96 using a protocol designed for live worms [4].

Table and Figure Legends

Table S1. Quantification and analysis of mitochondrial yield. Yields were calculated based on the comparison band intensities for the mitochondrial fraction (Mito) and the crude lysaste (Lys) shown in Figure S1.

Figure S1. Comparison of mitochondrial properties between different isolation techniques. (A) Immunoblots of mitochondria from crude lysate (Lys) and mitochondrial (Mito) fractions under different isolation protocols. Purity of fractions was assessed using mitochondrial (Mito) markers (ATP synthase subunit alpha -"CV-alpha" and a NDUFS3 – "CI"), a nuclear marker (Histone "H3"), and a cytoplasmic marker (α-tubulin, "Tub"). **(B)** Oxygen consumption ratio (OCR) (pmol/min/worm) measured from L4 staged worms with and without 1 hour collagenase 3 treatment. Error bars are SEM from N=40 wells, each containing 10 worms. Differences between isolation techniques were not significant (ns). Data shown is representative of two biological replicates. **(C)** Flow cytometric analysis of Mitotracker Red positive mitochondria from larval L1 and L4 worms using forward scatter (FSC) to estimate size (diameter, nm) and **(D)** side scatter (SSC) to measure "granularity". Medians are plotted. Differences within groups in **(C-D)** were either not significant or only marginally significant by Mann Whitney test. '*' = $p<0.05$. Error bars are SD.

Figure S2. Effects of depolarization on JC-9 dye retention in mitochondria and on morphology. (A) Contour plot showing distinct patterns for unlabeled mitochondria (Blue), JC-9 dye (10 μM) and the depolarizing agent Valinomycin (12 μM) alone (Red) and mitochondria, isolated from L4 stage worms, labeled with JC-9 and treated with Valinomycin (Orange). **(B)** Contour plot of isolated mitochondria from L1 stage worms labeled with JC-9 (Red) or with JC-9 and Valinomycin (Blue). **(C, C')** Histograms of particles (that are above-background fluorescence) and positive for Green, monomeric JC-9 signal **(C, Green)** and Red, aggregate JC-9 signal **(C', Red)**. Intensity of Green monomeric JC-9 signal **(C)** per particle is minimally influenced by the presence of valinomycin while the intensity of Red aggregate JC-9 signal **(C')** per particle decreases significantly when valinomycin is present. **(D)**. Medians for red and green fluorescence for data shown in C and C'. **(E)** Mitochondrial diameter (nm), derived from Forward scatter (FSC), increases (~1.2x) when mitochondria were depolarized (with valinomycin, **gray bars**) while **(F)** side scatter (SSC), mitochondria granularity, greatly increases upon depolarization (~2.9x). '*' = $p<0.05$ and '***' = $p<0.0001$. For **(C-F)** white bars represent 'polarized' mitochondria and grey bars represent 'depolarized'; N = 26274 for 'polarized' and N = 5455 for 'depolarized'. **(G)** Medians of fluorescence readings in the Green (white bars) and Red (grey bars) channels with respect to various combinations of dyes alone or mitochondrial treatments with dye and depolarizing agents. Labeled mitochondria are significantly higher (at least10-fold above controls) in fluorescence in the Green and Red channels than background fluorescence both with and without addition of the depolarization agent valinomycin (in Green signal from labeled mitochondria was 23x background fluorescence and with valinomycin, 13x; the Red signal from labeled mitochondria was 152x background and with valinomycin, 11x). 'x' = significance (signif.) $p<0.0001$ relative to 'JC9 alone', '#' = signif. $p<0.0001$ relative to 'JC9 alone & 12 μM Val.', '+' = signif. $p<0.0001$ relative to 'Unlabeled Mt' and '‡' = signif. $p<0.0001$ relative to 'Mt w/ JC9'. N = 8425 For 'JC9 alone', 17041 for 'JC9 & 12 μM Val.', 13052 for 'Unlab.

Mt', 5801 for 'Mt w/ JC9', and 3745 for 'Mt w/ JC9 & 12 µM Val.' Mann Whitney was performed to calculate the significance between any two medians.

Figure S3. Effects of depolarization on membrane potential, mitochondria diameter, and mitochondrial granularity. (A) Mitochondrial (Mito) diameter (in nm, computed from forward scatter, FSC) varies during development (1.2 ± 0.1, Mean ± Standard Deviation (SD), increase relative to the diameter of mitochondria isolated from Eggs) and mitochondria size also increases significantly following depolarization (grey bars) (1.2 ± 0.1, Mean ± SD, increase relative to the diameter of mitochondria compared to polarized, stage-matched counterparts). It is of note to mention, however, that the mitochondrial size variability we observe is minimal with respect to other accepted practices that alter mitochondrial morphology. For instance, addition of Ca^{2+} to isolated mitochondria causes the loss of $\Delta\psi$ and induction of mitochondrial permeability transition (MPT). This causes 'mitochondrial swelling' (1.6 ± 0.9, Mean ± SD, increase in diameter, calculated from EM images in [5,6]). Values plotted are medians. '#' = $p<0.0001$ relative to corresponding mitochondrial subtype in previous stage (e.g., L2 vs. L1), [1]= $p<0.0001$ relative to the other mitochondrial subtype within a stage (e.g., m^H vs. m^L in L1). **(B-D)** Distribution of $\Delta\psi$ **(B),** Mito size **(C)**, and Mito granularity **(D)**. The presence of mitochondria with high $\Delta\psi$ **(B)**, highly granular **(D)**, (called "m^H", yellow arrowheads) appears to account for the dramatic rise in median JC-9 ratio between L1-L3 stages (see **Figure 3A & 3B**). On the other hand, mitochondria with low $\Delta\psi$ **(B)** and low texture **(D)** are present through all stages ("m^L", blue arrowheads) and these represent the majority subtype in the Egg and L4-D2 stages. "Depol." = "depolarized". **(E)** Percent of depolarized mitochondria, defined by threshold described in **Figure S3F** below (and see **Figure 3C**), do not differ significantly between stages of development. Values are means computed from three biological replicates. Error bars are SEM. **(F-H)** Distributions of $\Delta\psi$ **(F)**, Mito size **(G)**, and Mito granularity **(H)** (SSC) when mitochondria are under depolarizing conditions. In **S3F**, the white line, "division point" represents the JC-9 ratio used to separate mitochondria into subsets with low and high $\Delta\psi$**. (I-J)** Mito size and **(J)** Mito granularity of both the m^H (grey bars) and m^L (white bars) throughout worm development. Values shown are medians. '#' = $p<0.0001$ relative to complementary mitochondrial subtype within a stage (e.g. m^H vs. m^L in L1), '‡' = $p<0.0001$ relative to 'polarized,' mitochondria within a stage. 'ns' = not significant. For 'polarized' mitochondria, N = 34280 for 'Eggs', 7963 for 'L1', 18586 for 'L2', 22313 for 'L3', 23497 for 'L4', 23476 for 'D1', and 45393 for 'D2'. For 'depolarized' mitochondria **(Figure S4A & S4E-H)**, N = 11613, 8137, 9965, 16035, 27394, 30069, and 29851 for Eggs – D2, respectively.

Figure S4. Morphological characterization of muscle mitochondria in transgenic lines. (A) Representative low-magnification micrograph of a whole transgenic worm expressing blue-fluorescent mitochondria (MLS::BFP) specifically in the muscle. Scale bar is 100 µm. **(B)** High magnification micrographs from all sections of a representative worm showing mitochondrial morphology and unlabeled, adjacent tissues. 'Ant' = anterior, 'med.1' = medial segment 1, 'med.2' = medial segment 2, and 'post' = posterior. 'p' = first pharyngeal bulb, 'ist' = isthmus, connecting the two pharyngeal bulbs, 'p'' = second pharyngeal bulb, 'int' = intestine, '*' = immature oocytes, 'a' = anus. Arrowheads mark hypodermis, also known as epidermis. Scale bar = 20 µm. **(C)** Micrograph of transgenic worm with blue-fluorescent mitochondria (Mito), as shown in **S4A & S4B**, co-labeled in live *C. elegans* with MitoTracker Green. TL = Transillumination. Scale bar is 20 µm. **(D)** Mito size and **(E)** Mito granularity from blue

[1]

fluorescently labeled muscle mitochondria (see **Figure 4A-B**). Values plotted are medians. **(F-H)** Distributions of $\Delta\psi$ (JC-9 ratio), Mito size, and Mito granularity of all worm mitochondria (red) and muscle mitochondria isolated from different transgenic lines expressing MLS::BFP (line #4, blue; line #8, orange; line #10, green). Of note, the size distribution of muscle mitochondria (see **Figures S4D & S4G**) from our flow measurements closely matches previously published distributions of *C. elegans* 'muscle' mitochondria obtained via confocal microscopy [7]. '***' = $p<0.0001$ relative to all tissues 'Total' mitochondria control, '‡' = $p<0.0001$ relative to 'polarized,' mitochondria within a stage. For 'polarized' mitochondria, N = 54839 for 'Total'. 1235 for 'Muscle(#4), 823 for 'Muscle(#8), and 618 for 'Muscle(#10)'.For 'depolarized' mitochondria N= 1176 for 'Total', 435 for 'Muscle(#4), 467 for 'Muscle(#8), and 392 for 'Muscle(#10).

Table S1

ANOVATwoWay (5/7/2016 06:21:18)

Descriptive Statistics

Disruption method

	N	Mean	SD	SEM	Variance	Missing	NonMissing
metal	4	0.32625	0.08901	0.04451	0.00792	0	4
glass	4	0.386	0.09461	0.04731	0.00895	0	4
glass col	4	0.40175	0.0593	0.02965	0.00352	0	4

stage

	N	Mean	SD	SEM	Variance	Missing	NonMissing
L1	6	0.37133	0.10233	0.04178	0.01047	0	6
L4	6	0.37133	0.06559	0.02678	0.0043	0	6

Overall

	N	Mean	SD	SEM	Variance	Missing	NonMissing
	12	0.37133	0.08194	0.02366	0.00671	0	12

Interaction

		N	Mean	SD	SEM	Variance	Missing	NonMissing
metal	L1	2	0.254	0.05374	0.038	0.00289	0	2
	L4	2	0.3985	7.07107E-4	5E-4	5E-7	0	2
glass	L1	2	0.467	0.02263	0.016	5.12E-4	0	2
	L4	2	0.305	0.0099	0.007	9.8E-5	0	2
glass col	L1	2	0.393	0.04667	0.033	0.00218	0	2
	L4	2	0.4105	0.0898	0.0635	0.00806	0	2

ANOVA

Overall ANOVA

	DF	Sum of Squares	Mean Square	F Value	P Value
Disruption method	2	0.01269	0.00635	2.7708	0.14049
stage	1	-1.04083E-17	-1.04083E-17	-4.5448E-15	1
Interaction	2	0.04743	0.02372	10.35525	0.01133
Model	5	0.06012	0.01202	5.25042	0.03375
Error	6	0.01374	0.00229	--	--
Corrected Total	11	0.07386	--	--	--

At the 0.05 level, the population means of **Disruption method** are **not significantly** different.
At the 0.05 level, the population means of **stage** are **not significantly** different.
At the 0.05 level, the interaction between **Disruption method** and **stage** is **significant**.

Means Comparisons

Tukey Test

Disruption method

	MeanDiff	SEM	q Value	Prob	Alpha	Sig	LCL	UCL
glass metal	0.05975	0.03384	2.49709	0.25846	0.05	0	-0.04408	0.16358
glass col metal	0.0755	0.03384	3.15532	0.14386	0.05	0	-0.02833	0.17933
glass col glass	0.01575	0.03384	0.65823	0.88954	0.05	0	-0.08808	0.11958

stage

	MeanDiff	SEM	q Value	Prob	Alpha	Sig	LCL	UCL
L4 L1	0	0.02763	0	1	0.05	0	-0.06761	0.06761

Sig equals 1 indicates that the difference of the means is significant at the 0.05 level.
Sig equals 0 indicates that the difference of the means is not significant at the 0.05 level.

Figure S1

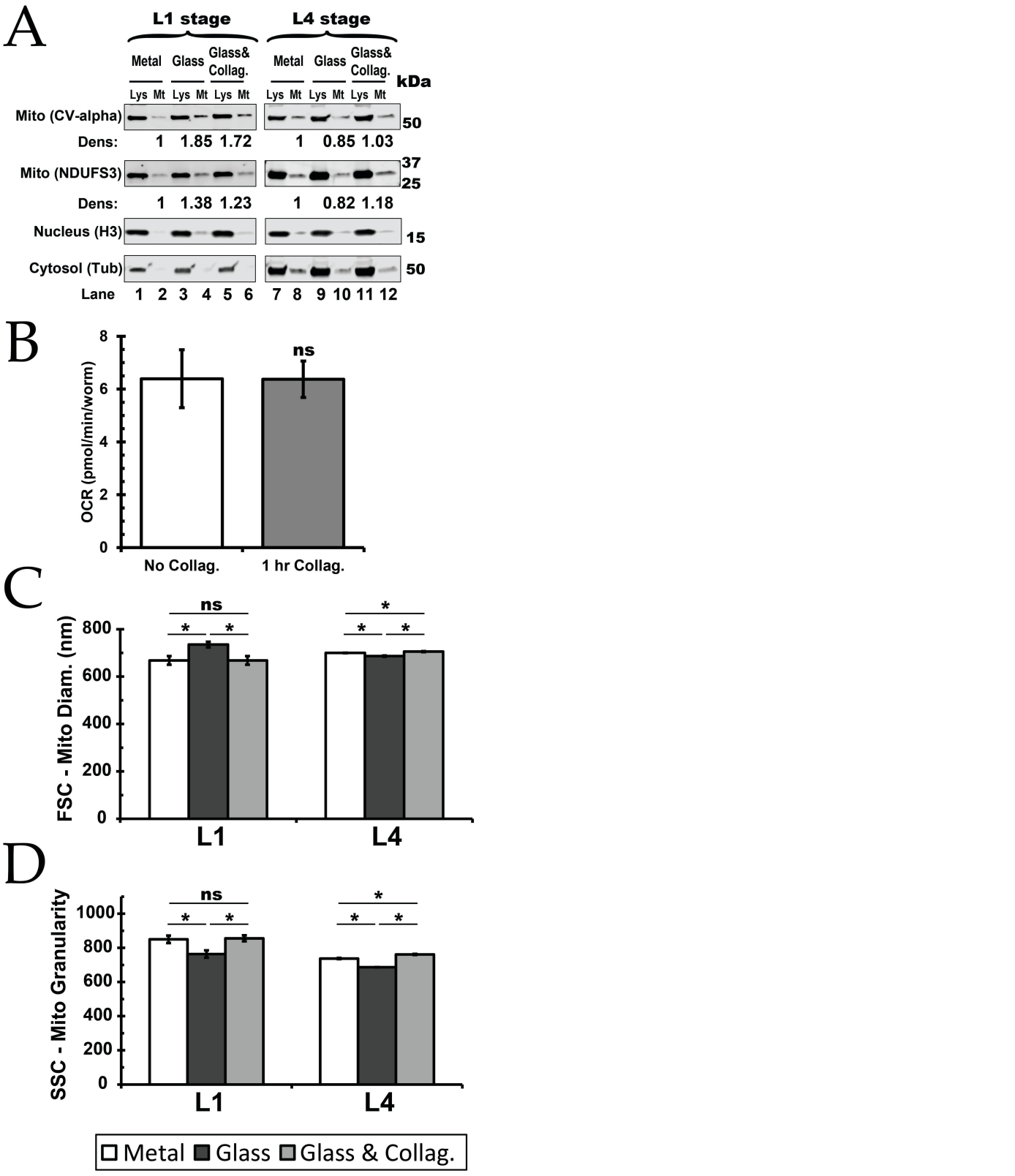
A
L1 stage
L4 stage
Metal
Glass
Glass& Collag.
Lys Mt Lys Mt Lys Mt Lys Mt Lys Mt Lys Mt
kDa
Mito (CV-alpha)
50
Dens: 1 1.85 1.72 1 0.85 1.03
Mito (NDUFS3)
37
25
Dens: 1 1.38 1.23 1 0.82 1.18
Nucleus (H3)
15
Cytosol (Tub)
50
Lane 1 2 3 4 5 6 7 8 9 10 11 12
B
OCR (pmol/min/worm)
ns
No Collag.
1 hr Collag.
C
FSC - Mito Diam. (nm)
ns
*
L1
L4
D
SSC - Mito Granularity
Metal
Glass
Glass & Collag.

Figure S2

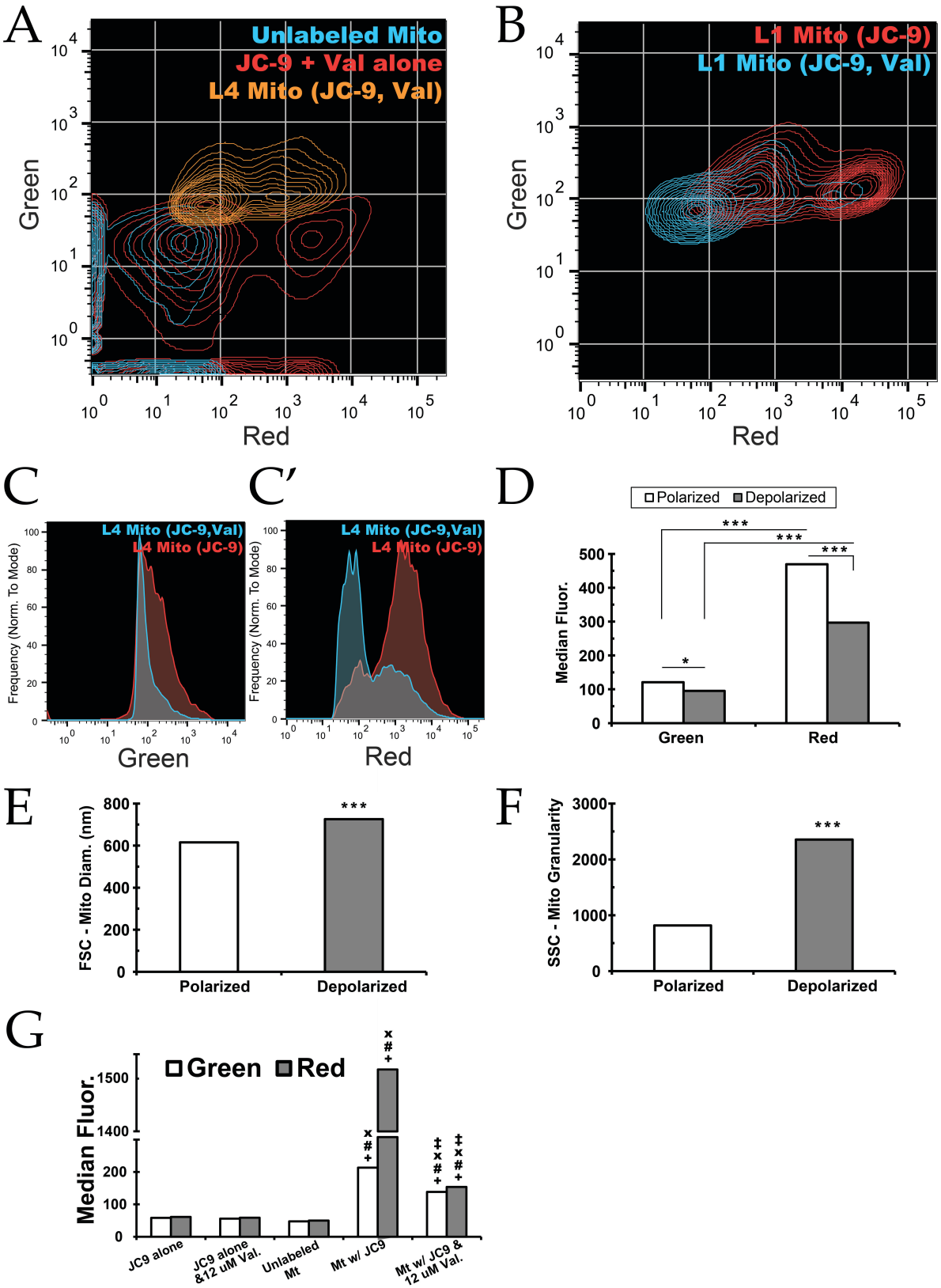
A
Unlabeled Mito
JC-9 + Val alone
L4 Mito (JC-9, Val)
Green
Red
B
L1 Mito (JC-9)
L1 Mito (JC-9, Val)
Green
Red
C
L4 Mito (JC-9,Val)
L4 Mito (JC-9)
Frequency (Norm. To Mode)
Green
C′
L4 Mito (JC-9,Val)
L4 Mito (JC-9)
Frequency (Norm. To Mode)
Red
D
Polarized
Depolarized
Median Fluor.
Green
Red
E
FSC - Mito Diam. (nm)
Polarized
Depolarized
F
SSC - Mito Granularity
Polarized
Depolarized
G
Green
Red
Median Fluor.
JC9 alone
JC9 alone &12 uM Val.
Unlabeled Mt
Mt w/ JC9
Mt w/ JC9 & 12 uM Val.

Figure S3

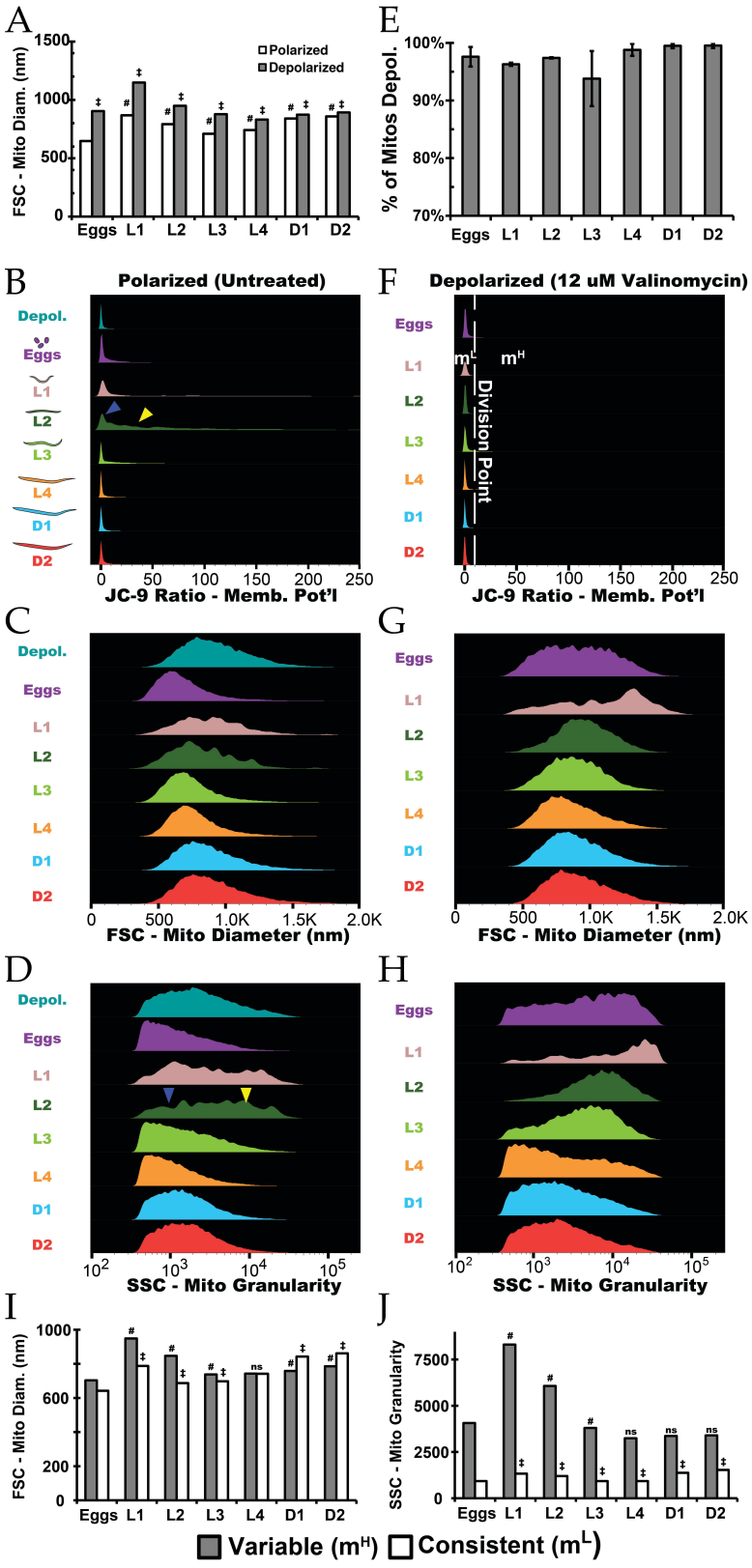
A
FSC - Mito Diam. (nm)
Polarized
Depolarized
Eggs L1 L2 L3 L4 D1 D2
E
% of Mitos Depol.
B
Polarized (Untreated)
Depol.
Eggs
L1
L2
L3
L4
D1
D2
JC-9 Ratio - Memb. Pot'l
F
Depolarized (12 uM Valinomycin)
Division Point
C
FSC - Mito Diameter (nm)
G
D
SSC - Mito Granularity
H
I
SSC - Mito Granularity
J
Variable (m^H)
Consistent (m^L)

Figure S4

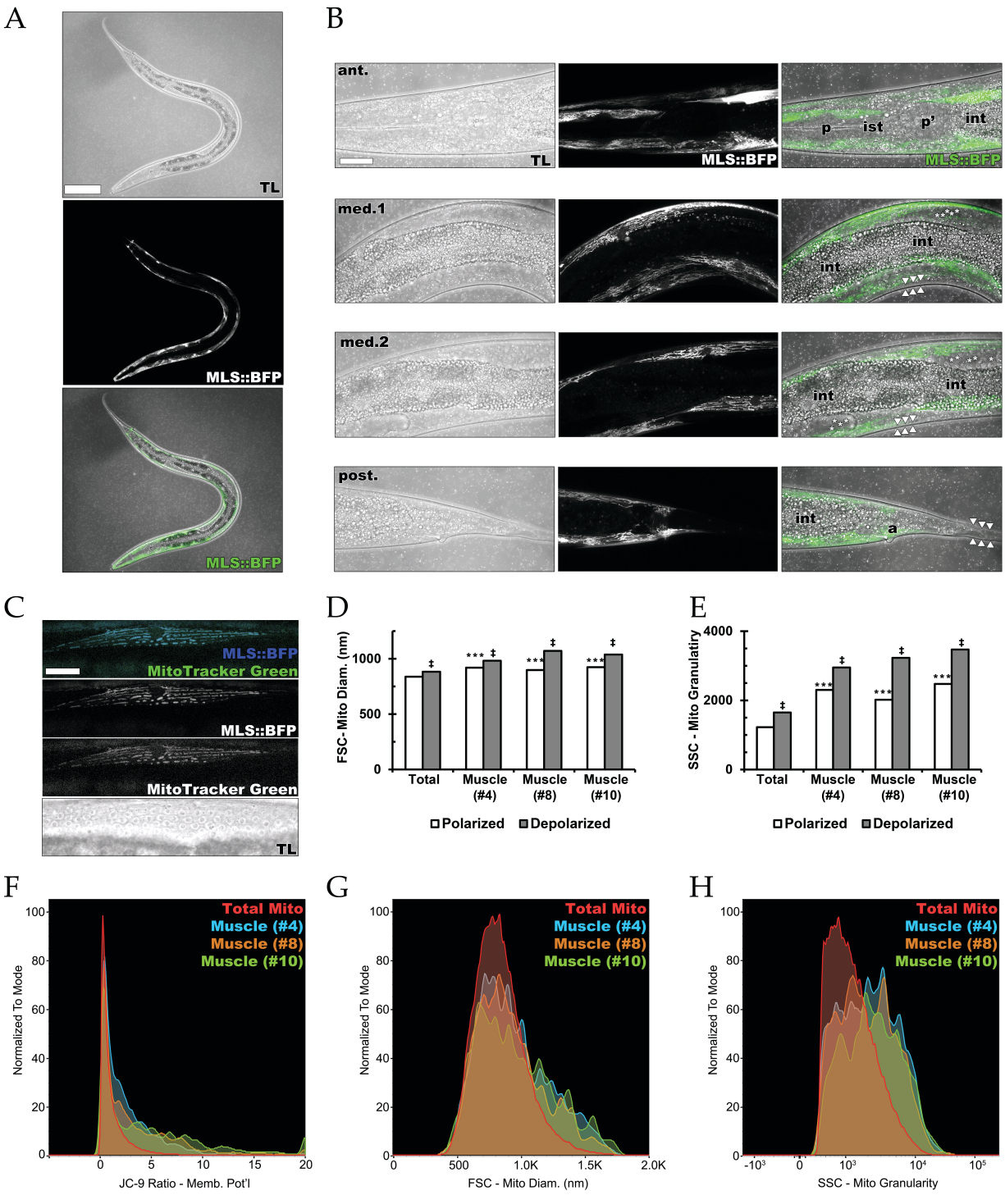
A
TL
MLS::BFP
MLS::BFP
B
ant.
TL
MLS::BFP
p
ist
p'
int
MLS::BFP
med.1
int
int
med.2
int
int
post.
int
a
C
MLS::BFP
MitoTracker Green
MLS::BFP
MitoTracker Green
TL
D
FSC- Mito Diam. (nm)
1000
500
0
Total
Muscle (#4)
Muscle (#8)
Muscle (#10)
Polarized
Depolarized
E
SSC - Mito Granularity
4000
2000
0
Total
Muscle (#4)
Muscle (#8)
Muscle (#10)
Polarized
Depolarized
F
Total Mito
Muscle (#4)
Muscle (#8)
Muscle (#10)
Normalized To Mode
JC-9 Ratio - Memb. Pot'l
G
Total Mito
Muscle (#4)
Muscle (#8)
Muscle (#10)
Normalized To Mode
FSC - Mito Diam. (nm)
H
Total Mito
Muscle (#4)
Muscle (#8)
Muscle (#10)
Normalized To Mode
SSC - Mito Granularity

References

(1) Chai, Y.; Li, W.; Feng, G.; Yang, Y.; Wang, X.; Ou, G. *Nat. Protoc.* **2012**, *7* (12), 2090–2102.

(2) Zeiser, E.; Frøkjær-Jensen, C.; Jorgensen, E.; Ahringer, J. *PLoS ONE* **2011**, *6* (5), e20082.

(3) Baird, N. A.; Douglas, P. M.; Simic, M. S.; Grant, A. R.; Moresco, J. J.; Wolff, S. C.; Yates, J. R.; Manning, G.; Dillin, A. *Science* **2014**, *346* (6207), 360–363.

(4) Houtkooper, R. H.; Mouchiroud, L.; Ryu, D.; Moullan, N.; Katsyuba, E.; Knott, G.; Williams, R. W.; Auwerx, J. *Nature* **2013**, *497* (7450), 451–457.

(5) Shinohara, Y.; Almofti, M. R.; Yamamoto, T.; Ishida, T.; Kita, F.; Kanzaki, H.; Ohnishi, M.; Yamashita, K.; Shimizu, S.; Terada, H. *Eur. J. Biochem.* **2002**, *269* (21), 5224–5230.

(6) Yamada, A.; Yamamoto, T.; Yamazaki, N.; Yamashita, K.; Kataoka, M.; Nagata, T.; Terada, H.; Shinohara, Y. *Mol. Cell. Proteomics* **2009**, *8* (6), 1265–1277.

(7) Head, B. P.; Zulaika, M.; Ryazantsev, S.; Bliek, A. M. van der. *Mol. Biol. Cell* **2011**, *22* (6), 831–841.